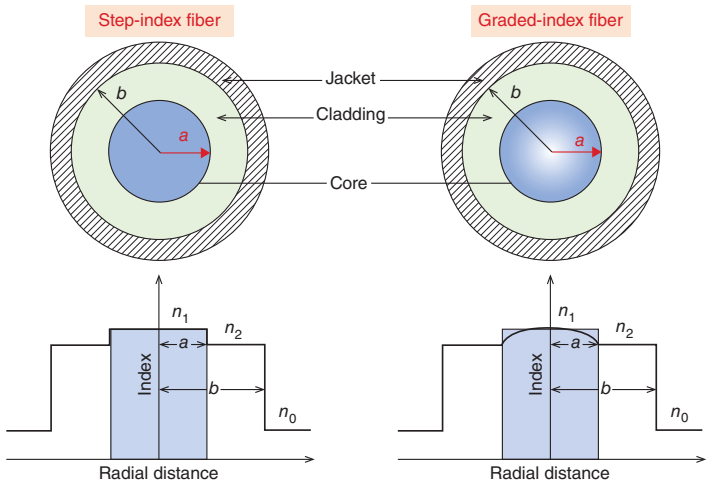

Figure 2.1: Cross sections and refractive-index profiles for step-index and graded-index fibers.

2.1.1 Step-Index Fibers

In Figure 2.2, a ray making an angle θ_i with the fiber's axis is incident at the core center. Because of refraction at the fiber–air interface, the ray bends toward the normal. The angle θ_r of the refracted ray is found from the Snell's law [12]

$$n_0 \sin\theta_i = n_1 \sin\theta_r, \tag{2.1.1}$$

where n_1 and n_0 are the refractive indices of the fiber's core and air, respectively. The refracted ray hits the core-cladding interface and is refracted again. However, refraction is possible only if the angle of incidence ϕ is less then the *critical angle* ϕ_c defined as

$$\sin\phi_c = n_2/n_1, \tag{2.1.2}$$

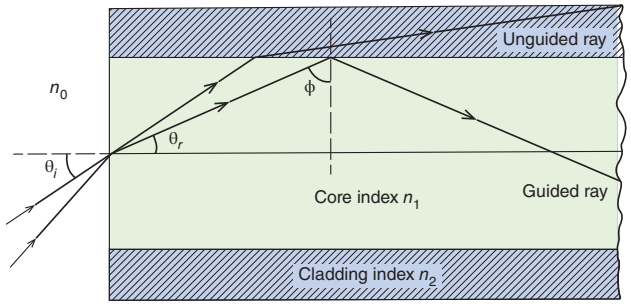

Figure 2.2: Light confinement through total internal reflection in step-index fibers. Rays for which $\phi < \phi_c$ are refracted out of the core.

where n_2 is the cladding's refractive index. For $\phi > \phi_c$, the ray undergoes total internal reflection at the core-cladding interface. As such reflections occur throughout the fiber's length, all rays with $\phi > \phi_c$ remain confined to the fiber core. This is the basic mechanism behind light confinement in optical fibers.

One can use Eqs. (2.1.1) and (2.1.2) to find the maximum angle that the incident ray should make with the fiber axis to remain confined inside the core. Noting that $\theta_r = \pi/2 - \phi_c$ for such a ray and substituting it in Eq. (2.1.1), we obtain

$$n_0 \sin\theta_i = n_1 \cos\phi_c = (n_1^2 - n_2^2)^{1/2}. \tag{2.1.3}$$

In analogy with lenses, $n_0 \sin\theta_i$ is known as the *numerical aperture* (NA) of the fiber. It represents the light-gathering capacity of an optical fiber. For $n_1 \simeq n_2$, the NA can be approximated by

$$\text{NA} = n_1(2\Delta)^{1/2}, \qquad \Delta = (n_1 - n_2)/n_1, \tag{2.1.4}$$

where Δ is the fractional index change at the core-cladding interface. Clearly, Δ should be made as large as possible in order to couple maximum light into the fiber. However, such fibers are not useful for optical communications because of a phenomenon known as multipath or *modal dispersion* (fiber modes are introduced in Section 2.2).

Multipath dispersion can be understood from Figure 2.2, where different rays travel along paths of different lengths. As a result, these rays disperse in time at the output end of the fiber even if they were coincident at the input end and traveled at the same speed inside the fiber. As a result, a short pulse (called an impulse) would broaden considerably inside the fiber. One can estimate the extent of pulse broadening by considering the shortest and longest ray paths. The shortest path occurs for $\theta_i = 0$ and is just equal to the fiber length L. The longest path occurs for θ_i given in Eq. (2.1.3) and has a length $L/\sin\phi_c$. Using $v = c/n_1$ for the speed of propagation, the time delay is given by

$$\Delta T = \frac{n_1}{c}\left(\frac{L}{\sin\phi_c} - L\right) = \frac{L}{c}\frac{n_1^2}{n_2}\,\Delta. \tag{2.1.5}$$

The time delay between the two rays taking the shortest and longest paths is a measure of broadening experienced by an impulse launched at the fiber's input end.

We can relate ΔT to the information-carrying capacity of a fiber measured through the bit rate B. Although a precise relation between B and ΔT depends on many details, such as the pulse shape, it is clear intuitively that ΔT should be less than the allocated bit slot ($T_B = 1/B$). Thus, a rough estimate of the bit rate is obtained from the condition $B\Delta T < 1$. By using Eq. (2.1.5), we obtain

$$BL < \frac{n_2}{n_1^2}\frac{c}{\Delta}. \tag{2.1.6}$$

As an illustration, consider an unclad glass fiber with $n_1 = 1.5$ and $n_2 = 1$. The bit rate-distance product of such a fiber is limited to $BL < 0.4$ (Mb/s)-km. Considerable improvement occurs for cladded fibers with a small index step. Optical fibers used for telecommunication applications are designed with $\Delta < 0.01$. As an example, $BL < 100$ (Mb/s)-km for $\Delta = 2 \times 10^{-3}$. Such fibers can transfer data at a bit rate of 10 Mb/s over distances up to 10 km and are suitable for some local-area networks.

2.1.2 Graded-Index Fibers

The refractive index of the core in a GRIN fiber y from its maximum value n_1 at the core center to its mi erface.

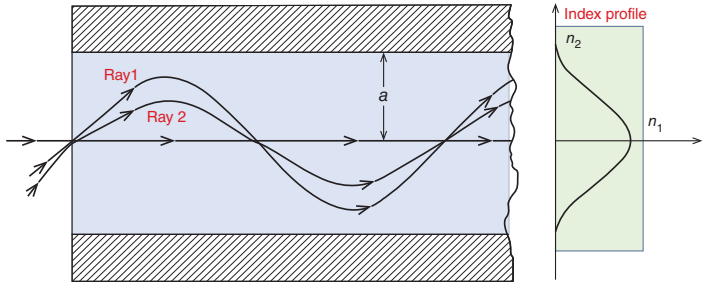

Figure 2.3: Ray trajectories in a graded-index fiber.

Most GRIN fibers are designed to have a nearly quadratic decrease and are analyzed by using the α-profile given by

$$n(\rho) = \begin{cases} n_1[1 - \Delta(\rho/a)^\alpha]; & \rho < a, \\ n_1(1 - \Delta) = n_2 \ ; & \rho \geq a. \end{cases} \tag{2.1.7}$$

The parameter α determines the shape of the index profile. A step-index profile is approached in the limit of large α. A parabolic-index fiber corresponds to $\alpha = 2$.

It is easy to understand qualitatively why intermodal or multipath dispersion is reduced for GRIN fibers. Figure 2.3 shows schematically paths for three different rays. Similar to the case of step-index fibers, the path is longer for more oblique rays. However, the ray velocity changes along the path because of variations in the refractive index. More specifically, the ray propagating along the fiber axis takes the shortest path but travels slowest as the refractive index is largest along this path. Oblique rays have a large part of their path in a medium of lower refractive index, where they travel faster. It is thus possible for all rays to arrive together at the output end for a suitable choice of the refractive-index profile.

Geometrical optics can be used to show that a parabolic-index profile ($\alpha = 2$) leads to nondispersive propagation within the *paraxial approximation*. The trajectory of a paraxial ray is obtained by solving the ray equation [12]

$$\frac{d^2\rho}{dz^2} = \frac{1}{n}\frac{dn}{d\rho}, \tag{2.1.8}$$

where ρ is the radial distance of the ray from the axis. By using Eq. (2.1.7) for $\rho < a$ with $\alpha = 2$, Eq. (2.1.8) reduces to an equation of harmonic oscillator and has the general solution

$$\rho = \rho_0 \cos(pz) + (\rho_0'/p)\sin(pz), \tag{2.1.9}$$

where $p = \sqrt{2\Delta}/a$ and ρ_0 and ρ_0' are the position and the direction of the input ray, respectively. Equation (2.1.9) shows that all rays recover their initial positions and directions at distances $z = 2m\pi/p$, where m is an integer (see Figure 2.3). Such a restoration of input pulses is useful for telecom applications.

The preceding conclusion holds only within the paraxial and the geometrical-optics approximations, both of which must be relaxed for practical fibers. Intermodal dispersion in GRIN fibers has been studied extensively [13]. The quantity $\Delta T/L$, where ΔT is the maximum multipath delay in a fiber of length L, is found to vary considerably with α. Figure 2.4 shows this variation for $n_1 = 1.5$ and $\Delta = 0.01$. The minimum dispersion occurs for $\alpha = 2(1 - \Delta)$ and depends on Δ as

$$\Delta T/L = n_1\Delta^2/8c. \tag{2.1.10}$$

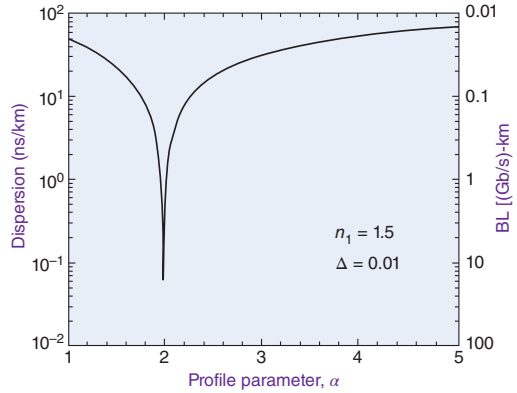

Figure 2.4: Variation of intermodal dispersion $\Delta T/L$ with the profile parameter α for a graded-index fiber. The scale on the right shows the corresponding bit rate-distance product.

The limiting bit rate-distance product is obtained by using the criterion $\Delta T < 1/B$ and is given by

$$BL < 8c/n_1\Delta^2. \tag{2.1.11}$$

The right scale in Figure 2.4 shows the BL product as a function of α. GRIN fibers with a suitably optimized index profile can transfer data at a bit rate of 100 Mb/s over distances of up to 100 km. Indeed, the first generation of lightwave systems used GRIN fibers. Further improvement was possible only by using the so-called single-mode fibers. Geometrical optics cannot be used for such fibers.

Although GRIN fibers are rarely used for long-haul links, the use of such fibers made with plastics is a viable option for data-link applications. Plastic fibers exhibit high losses (>20 dB/km) but can still be used to transmit data at bit rates of up to 10 Gb/s over short distances (1 km or less) because of their GRIN profile (see Section 2.7.2 for further details).

2.2 Wave Propagation

In this section, we consider propagation of electromagnetic waves inside step-index fibers. We introduce Maxwell's equations in Section 2.2.1 and solve them in Section 2.2.2 to obtain optical modes that remain guided inside an optical fiber. Section 2.2.3 focuses on how an optical fiber can be designed to support only a single mode and describes the properties of such single-mode fibers.

2.2.1 Maxwell's Equations

Like all electromagnetic phenomena, propagation of optical fields in fibers is governed by *Maxwell's equations*. For a dielectric medium without free charges, these equations take the form [14] (in SI units; see Appendix A)

$$\nabla \times \mathbf{E} = -\partial\mathbf{B}/\partial t, \qquad \nabla \cdot \mathbf{D} = 0, \tag{2.2.1}$$

$$\nabla \times \mathbf{H} = \partial\mathbf{D}/\partial t, \qquad \nabla \cdot \mathbf{B} = 0, \tag{2.2.2}$$

of V supports many modes. A rough estimate of the number of modes for such a multimode fiber is given by $V^2/2$ [13]. For example, a multimode fiber with $a = 25\ \mu$m and $\Delta = 5 \times 10^{-3}$ has $V = 18$ at $\lambda = 1.3\ \mu$m and it supports about 162 modes. However, the number of modes decreases rapidly as V is reduced. As seen in Figure 2.5, a fiber with $V = 5$ supports seven modes. Below a certain value of V, all modes except the HE_{11} mode reach cutoff. Such fibers support a single mode and are called single-mode fibers. The properties of single-mode fibers are described in this section. Multimode fibers are covered in Chapter 11 devoted to the technique of space-division multiplexing.

2.2.3 Single-Mode Fibers

Single-mode fibers support only the HE_{11} mode, also known as the fundamental mode of the fiber. The fiber is designed such that all higher-order modes are cut off at the operating wavelength. As seen in Figure 2.5, the V parameter determines the number of modes supported by a fiber and only the HE_{11} mode exists for $V < 2.4$.

Single-Mode Condition

The *single-mode condition* is determined by the value of V at which the TE_{01} and TM_{01} modes reach cutoff (see Figure 2.5). The eigenvalue equations for these two modes can be obtained by setting $m = 0$ in Eq. (2.2.28) and are given by

$$pJ_0(pa)K_0'(qa) + qJ_0'(pa)K_0(qa) = 0, \tag{2.2.32}$$

$$pn_2^2 J_0(pa)K_0'(qa) + qn_1^2 J_0'(pa)K_0(qa) = 0. \tag{2.2.33}$$

A mode reaches cutoff when $q = 0$. Since $pa = V$ when $q = 0$, the cutoff condition for both modes is simply given by $J_0(V) = 0$. The smallest value of V for which $J_0(V) = 0$ is 2.405. A fiber designed such that $V < 2.405$ supports only the fundamental HE_{11} mode. This is the single-mode condition.

We can use Eq. (2.2.29) to estimate the core radius of single-mode fibers used for lightwave systems. For the operating wavelength range 1.3–1.6 μm, the fiber is generally designed to become single mode for $\lambda > 1.2\ \mu$m. By using $\lambda = 1.2\ \mu$m, $n_1 = 1.45$, and $\Delta = 3 \times 10^{-3}$, Eq. (2.2.29) shows that $V < 2.405$ for a core radius $a < 4\ \mu$m. The required core radius can be increased by decreasing Δ. Indeed, most telecommunication fibers are designed with $a < 5\ \mu$m.

The mode index $\bar{n}$ can be obtained by using Eq. (2.2.31) or

$$\bar{n} = n_2 + b(n_1 - n_2) \approx n_2(1 + b\Delta), \tag{2.2.34}$$

where b is estimated from Figure 2.5 for the specific value of V for the fiber. The analytic approximation,

$$b(V) \approx (1.1428 - 0.9960/V)^2, \tag{2.2.35}$$

is accurate to within 0.2% for V in the range of 1.5–2.5.

The spatial distribution of the fundamental mode is obtained from Eqs. (2.2.22) through (2.2.27). The axial components E_z and H_z are quite small for $\Delta \ll 1$, i.e., the HE_{11} mode is almost linearly polarized in weakly guiding fibers. It is also denoted as LP_{01} mode [17]. One of the transverse components can be taken as zero for a linearly polarized mode. If we set $E_y = 0$, the E_x component of the electric field for the HE_{11} mode is given by [10]

$$E_x = E_0 \begin{cases} [J_0(p\rho)/J_0(pa)]\exp(i\beta z)\ ; & \rho \le a, \\ [K_0(q\rho)/K_0(qa)]\exp(i\beta z); & \rho > a, \end{cases} \tag{2.2.36}$$

Spot Size

Since the field distribution given in Eq. (2.2.36) is cumbersome to use in practice, it is often approximated by a Gaussian distribution of the form

$$E_x = A\exp(-\rho^2/w^2)\exp(i\beta z), \tag{2.2.38}$$

where w is the *field radius* and is referred to as the *spot size*. It is determined by fitting the exact distribution to the Gaussian function or by following a variational procedure [19]. Figure 2.7 shows the dependence of w/a on the V parameter. A comparison of the actual field distribution with the fitted Gaussian is also shown for $V = 2.4$. The quality of fit is generally quite good for values of V in the neighborhood of 2. The spot size w can be determined from Figure 2.7. It can also be determined from an analytic approximation accurate to within 1% for $1.2 < V < 2.4$ and given by [19]

$$w/a \approx 0.65 + 1.619V^{-3/2} + 2.879V^{-6}. \tag{2.2.39}$$

The mode area, defined as $a_m = \pi w^2$, is an important parameter for optical fibers as it determines how tightly light is confined to the core.

The fraction of the power contained in the core can be obtained by using Eq. (2.2.38) and is given by the *confinement factor*

$$\Gamma = \frac{P_{\text{core}}}{P_{\text{total}}} = \frac{\int_0^a |E_x|^2 \rho\, d\rho}{\int_0^\infty |E_x|^2 \rho\, d\rho} = 1 - \exp\left(-\frac{2a^2}{w^2}\right). \tag{2.2.40}$$

Equations (2.2.39) and (2.2.40) determine the fraction of the mode power contained inside the core for a given value of V. Although nearly 75% of the mode power resides in the core for $V = 2$, this percentage drops down to 20% for $V = 1$. For this reason, most single-mode fibers are designed to operate in the range $2 < V < 2.4$.

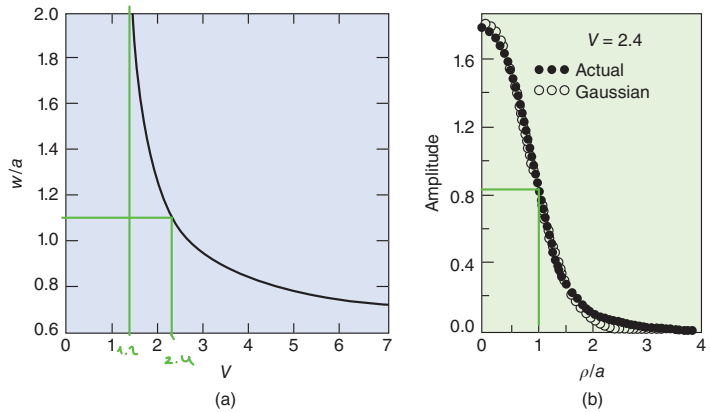

Figure 2.7: (a) Normalized spot size w/a as a function of the V parameter obtained by fitting the fundamental fiber mode to a Gaussian distribution; (b) quality of fit for $V = 2.4$. Modified from Marcuse [19].

2.3 Dispersion in Single-Mode Fibers

→ Dalga formunun bozulmasi

It was seen in Section 2.1 that intermodal dispersion in multimode fibers can lead to considerable broadening of optical pulses (∼ 10 ns/km). In the modal description, the broadening is related to different speeds associated with different modes. The main advantage of single-mode fibers is that intermodal dispersion disappears simply because the entire energy of a pulse is transported by a single mode. However, pulse broadening does not disappear altogether because the effective index $\bar{n}(\omega)$ of the fundamental mode depends on frequency because of chromatic dispersion. As a result, different spectral components of the pulse travel at slightly different group velocities, a phenomenon referred to as *group-velocity dispersion* (GVD) or intramodal dispersion. Intramodal dispersion has two contributions known as material dispersion and waveguide dispersion. We consider both of them and discuss how the GVD limits the performance of lightwave systems employing single-mode fibers.

2.3.1 Group-Velocity Dispersion

Consider an optical pulse launched into a single-mode fiber of length L. A specific spectral component at the frequency ω would arrive at the output end of the fiber after a time delay $T = L/v_g$, where the *group velocity* v_g is defined as [12]

$$v_g = (d\beta/d\omega)^{-1}. \tag{2.3.1}$$

By using $\beta(\omega) = \bar{n}k_0 = \bar{n}(\omega)\omega/c$ in Eq. (2.3.1), we can show that $v_g = c/\bar{n}_g$, where $\bar{n}_g$ is the *group index* given by

$$\bar{n}_g = \bar{n} + \omega(d\bar{n}/d\omega)\ . \tag{2.3.2}$$

The frequency dependence of the group velocity leads to pulse broadening because different spectral components of a pulse do not arrive simultaneously at the fiber's output end. If $\Delta\omega$ is the spectral width of the pulse, the extent of pulse broadening for a fiber of length L is governed by

$$\Delta T = \frac{dT}{d\omega}\Delta\omega = \frac{d}{d\omega}\left(\frac{L}{v_g}\right)\Delta\omega = L\frac{d^2\beta}{d\omega^2}\Delta\omega = L\beta_2\Delta\omega, \tag{2.3.3}$$

where Eq. (2.3.1) was used. The parameter $\beta_2 = d^2\beta/d\omega^2$ is known as the GVD parameter. It determines how much an optical pulse would broaden on propagation inside a single-mode fiber.

In some optical communication systems, the frequency spread $\Delta\omega$ is set by the range of wavelengths $\Delta\lambda$ emitted by an optical source. By using $\omega = 2\pi c/\lambda$ and $\Delta\omega = (-2\pi c/\lambda^2)\Delta\lambda$, Eq. (2.3.3) can be written as

$$\Delta T = \frac{d}{d\lambda}\left(\frac{L}{v_g}\right)\Delta\lambda = DL\Delta\lambda, \tag{2.3.4}$$

where D is the *dispersion parameter* defined as [units: ps/(km-nm)]

$$D = \frac{d}{d\lambda}\left(\frac{1}{v_g}\right) = -\frac{2\pi c}{\lambda^2}\beta_2. \tag{2.3.5}$$

The effect of dispersion on the bit rate B can be estimated by using the criterion $B\Delta T < 1$ in a manner similar to that used in Section 2.1. By using ΔT from Eq. (2.3.4), this condition becomes

$$BL|D|\Delta\lambda < 1. \tag{2.3.6}$$

Equation (2.3.6) provides an order-of-magnitude estimate of the BL product for single-mode fibers. For standard silica fibers, D is relatively small in the wavelength region near 1.3 μm [$D \sim 1$ ps/(km-nm)]. For a semiconductor laser, the spectral width $\Delta\lambda$ is 2–4 nm even when the laser operates in several longitudinal modes. The BL product of such lightwave systems can exceed 100 (Gb/s)-km. Indeed, the second-generation systems appeared around 1985 and operated at 1.3 μm with a bit rate of up to 2 Gb/s and a repeater spacing of 40–50 km. Moreover, the BL product exceeded 1 (Tb/s)-km when single-mode semiconductor lasers were used to reduce $\Delta\lambda$ below 1 nm.

The operated wavelength shifted to 1.55 μm for the third generation of lightwave systems. The dispersion parameter D changes considerably when the operating wavelength is shifted from 1.3 μm. The wavelength dependence of D is governed by the frequency dependence of the mode index $\bar{n}$. From Eq. (2.3.5), D can be written as

$$D = -\frac{2\pi c}{\lambda^2}\frac{d}{d\omega}\left(\frac{1}{v_g}\right) = -\frac{2\pi}{\lambda^2}\left(2\frac{d\bar{n}}{d\omega} + \omega\frac{d^2\bar{n}}{d\omega^2}\right), \tag{2.3.7}$$

where Eq. (2.3.2) was used. If we substitute $\bar{n}$ from Eq. (2.2.34) and use Eq. (2.2.29), D can be written as the sum of two terms,

$$D = D_M + D_W, \tag{2.3.8}$$

where the *material dispersion* D_M and the *waveguide dispersion* D_W are given by

$$D_M = -\frac{2\pi}{\lambda^2}\frac{dn_{2g}}{d\omega} = \frac{1}{c}\frac{dn_{2g}}{d\lambda}, \tag{2.3.9}$$

$$D_W = -\frac{2\pi\Delta}{\lambda^2}\left[\frac{n_{2g}^2}{n_2\omega}\frac{Vd^2(Vb)}{dV^2} + \frac{dn_{2g}}{d\omega}\frac{d(Vb)}{dV}\right]. \tag{2.3.10}$$

Here n_{2g} is the group index of the cladding material and the parameters V and b are given by Eqs. (2.2.29) and (2.2.31), respectively. In Eqs. (2.3.8) through (2.3.10), the parameter Δ is assumed to be frequency independent. A third term known as differential material dispersion should be added to Eq. (2.3.8) when $d\Delta/d\omega \neq 0$. Its contribution is, however, negligible in practice.

2.3.2 Material Dispersion

Material dispersion occurs because the refractive index of silica glass, the material used for making fibers, depends on ω. On a fundamental level, the origin of material dispersion is related to the atomic resonance frequencies at which the material absorbs electromagnetic radiation. Far from such resonances, the refractive index is well approximated by the *Sellmeier equation* [20]

$$n^2(\omega) = 1 + \sum_{j=1}^{M}\frac{B_j\omega_j^2}{\omega_j^2 - \omega^2}, \tag{2.3.11}$$

where ω_j is the resonance frequency and B_j is the oscillator strength. The sum in Eq. (2.3.11) extends over all material resonances that contribute in the frequency range of interest. In the case of optical fibers, the parameters B_j and ω_j are obtained empirically by fitting the measured dispersion curves to Eq. (2.3.11) with $M = 3$. They depend on the amount of dopants and have been tabulated for several kinds of fibers [7]. For pure silica, these parameters are found to be $B_1 = 0.6961663$, $B_2 = 0.4079426$, $B_3 = 0.8974794$, $\lambda_1 = 0.0684043$ μm, $\lambda_2 = 0.1162414$ μm, and $\lambda_3 = 9.896161$ μm, where $\lambda_j = 2\pi c/\omega_j$ with $j = 1$ to 3 [20]. The group index $n_g = n + \omega(dn/d\omega)$ can be obtained by using these parameter values.

Optical Sources with a Large Spectral Width

This case corresponds to $V_\omega \gg 1$ in Eq. (2.4.23). Consider first the case of a lightwave system operating away from the zero-dispersion wavelength so that the β_3 term can be neglected. The effects of frequency chirp are negligible for sources with a large spectral width. By setting $C = 0$ in Eq. (2.4.23), we obtain

$$\sigma^2 = \sigma_0^2 + (\beta_2 L \sigma_\omega)^2 \equiv \sigma_0^2 + (DL\sigma_\lambda)^2, \tag{2.4.24}$$

where σ_λ is the RMS source spectral width in wavelength units. The output pulse width is thus given by

$$\sigma = (\sigma_0^2 + \sigma_D^2)^{1/2}, \tag{2.4.25}$$

where $\sigma_D \equiv |D|L\sigma_\lambda$ provides a measure of dispersion-induced broadening.

We can relate σ to the bit rate by using the criterion that the broadened pulse should remain inside the allocated bit slot, $T_B = 1/B$, where B is the bit rate. A commonly used criterion is $\sigma \le T_B/4$; for Gaussian pulses at least 95% of the pulse energy then remains within the bit slot. The limiting bit rate is given by $4B\sigma \le 1$. In the limit $\sigma_D \gg \sigma_0$, $\sigma \approx \sigma_D = |D|L\sigma_\lambda$, and the condition becomes

$$BL|D|\sigma_\lambda \le \frac{1}{4}. \tag{2.4.26}$$

This condition should be compared with Eq. (2.3.6) obtained heuristically; the two become identical if we interpret $\Delta\lambda$ as $4\sigma_\lambda$ in Eq. (2.3.6).

For a lightwave system operating exactly at the zero-dispersion wavelength, $\beta_2 = 0$ in Eq. (2.4.23). By setting $C = 0$ as before and assuming $V_\omega \gg 1$, Eq. (2.4.23) can be approximated by

$$\sigma^2 = \sigma_0^2 + \frac{1}{2}(\beta_3 L \sigma_\omega^2)^2 \equiv \sigma_0^2 + \frac{1}{2}(SL\sigma_\lambda^2)^2, \tag{2.4.27}$$

where Eq. (2.3.13) was used to relate β_3 to the dispersion slope S. The output pulse width is thus given by Eq. (2.4.25) but now $\sigma_D \equiv |S|L\sigma_\lambda^2/\sqrt{2}$. As before, we can relate σ to the limiting bit rate by the condition $4B\sigma \le 1$. When $\sigma_D \gg \sigma_0$, the limitation on the bit rate is governed by

$$BL|S|\sigma_\lambda^2 \le 1/\sqrt{8}\,. \tag{2.4.28}$$

This condition should be compared with Eq. (2.3.14) obtained heuristically by using simple physical arguments.

As an example, consider the case of a light-emitting diode with $\sigma_\lambda \approx 15$ nm. By using $D = 17$ ps/(km-nm) at 1.55 μm, Eq. (2.4.26) yields $BL < 1$ (Gb/s)-km. However, if the system is designed to operate at the zero-dispersion wavelength, BL can be increased to 20 (Gb/s)-km for a typical value $S = 0.08$ ps/(km-nm^2).

Optical Sources with a Small Spectral Width

This case corresponds to $V_\omega \ll 1$ in Eq. (2.4.23). As before, if we neglect the β_3 term and set $C = 0$, Eq. (2.4.23) can be approximated by

$$\sigma^2 = \sigma_0^2 + (\beta_2 L/2\sigma_0)^2 \equiv \sigma_0^2 + \sigma_D^2. \tag{2.4.29}$$

A comparison with Eq. (2.4.25) reveals a major difference between the two cases. In the case of a narrow source spectrum, dispersion-induced broadening depends on the initial width σ_0, whereas it is independent of σ_0 when the spectral width of the optical source dominates. In fact, σ can be minimized by choosing an optimum value of σ_0. The minimum value of σ is found to occur for

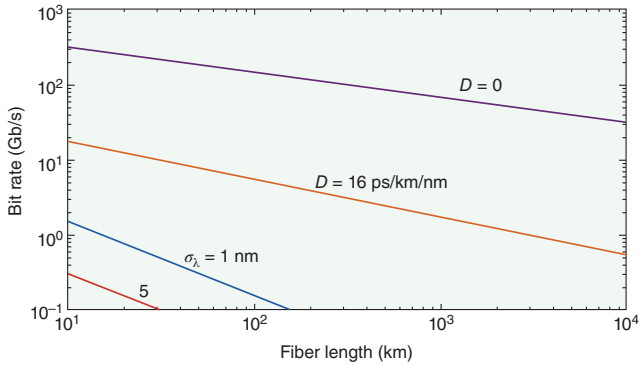

Figure 2.12: Limiting bit rate of single-mode fibers as a function of the fiber length for $\sigma_\lambda = 0$, 1, and 5 nm. The case $\sigma_\lambda = 0$ corresponds to the case of an optical source whose spectral width is much smaller than the bit rate.

$\sigma_0 = \sigma_D = (|\beta_2|L/2)^{1/2}$ and is given by $\sigma = (|\beta_2|L)^{1/2}$. The limiting bit rate is obtained by using $4B\sigma \le 1$ and leads to the condition

$$B\sqrt{|\beta_2|L} \le \frac{1}{4}. \tag{2.4.30}$$

The main difference from Eq. (2.4.26) is that B scales as $L^{-1/2}$ rather than L^{-1}. Figure 2.12 compares the decrease in the bit rate with increasing L for $\sigma_\lambda = 0$, 1, and 5 nm using $D = 16$ ps/(km-nm). Equation (2.4.30) was used in the case $\sigma_\lambda = 0$.

For a lightwave system operating close to the zero-dispersion wavelength, $\beta_2 \approx 0$ in Eq. (2.4.23). Using $V_\omega \ll 1$ and $C = 0$, the pulse width is then given by

$$\sigma^2 = \sigma_0^2 + (\beta_3 L/4\sigma_0^2)^2/2 \equiv \sigma_0^2 + \sigma_D^2. \tag{2.4.31}$$

Similar to the case of Eq. (2.4.29), σ can be minimized by optimizing the input pulse width σ_0. The minimum value of σ occurs for $\sigma_0 = (|\beta_3|L/4)^{1/3}$ and is given by

$$\sigma = \left(\frac{3}{2}\right)^{1/2} (|\beta_3|L/4)^{1/3}. \tag{2.4.32}$$

The limiting bit rate is obtained by using the condition $4B\sigma \le 1$, or

$$B(|\beta_3|L)^{1/3} \le 0.324. \tag{2.4.33}$$

The dispersive effects are most forgiving in this case. When $\beta_3 = 0.1$ ps^3/km, the bit rate can be as large as 150 Gb/s for $L = 100$ km. It decreases to only about 70 Gb/s even when L increases by a factor of 10 because of the $L^{-1/3}$ dependence of the bit rate on the fiber length. The dashed line in Figure 2.12 shows this dependence by using Eq. (2.4.33) with $\beta_3 = 0.1$ ps^3/km. Clearly, the performance of a lightwave system can be improved considerably by operating it near the zero-dispersion wavelength of the fiber and using optical sources with a relatively narrow spectral width.

Effect of Frequency Chirp

The input pulse in all preceding cases has been assumed to be an unchirped Gaussian pulse. In practice, optical pulses are often non-Gaussian and may exhibit considerable chirp. A super-Gaussian

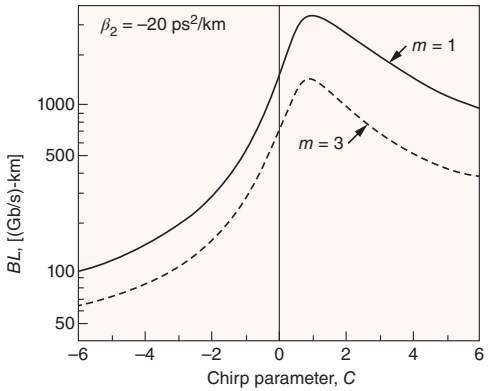

Figure 2.13: Dispersion-limited BL product as a function of the chirp parameter for Gaussian (solid curve) and super-Gaussian (dashed curve) input pulses. Source: Modified from Agrawal and Potasek [36].

model has been used to study the bit-rate limitation imposed by fiber dispersion for an NRZ-format bit stream [36]. In this model, Eq. (2.4.10) is replaced by

$$A(0,T) = A_0 \exp\left[-\frac{1+iC}{2}\left(\frac{t}{T_0}\right)^{2m}\right], \tag{2.4.34}$$

where the parameter m controls the pulse shape. Chirped Gaussian pulses correspond to $m = 1$. For large value of m, the pulse becomes nearly rectangular with sharp leading and trailing edges. The output pulse shape can be obtained by solving Eq. (2.4.9) numerically. The limiting bit rate-distance product BL is found by requiring that the RMS pulse width does not increase above a tolerable value. Figure 2.13 shows the BL product as a function of the chirp parameter C for Gaussian ($m = 1$) and super-Gaussian ($m = 3$) input pulses. In both cases, the fiber length L at which the pulse broadens by 20% was obtained for $T_0 = 125$ ps and $\beta_2 = -20$ ps^2/km. As expected, the BL product is smaller for super-Gaussian pulses because such pulses broaden more rapidly than Gaussian pulses. The BL product is reduced dramatically for negative values of the chirp parameter C. This is due to enhanced broadening occurring when $\beta_2 C$ is positive (see Figure 2.11). Unfortunately, C is generally negative for directly modulated semiconductor lasers with a typical value of -6 at 1.55 μm. As $BL < 100$ (Gb/s)-km under such conditions, the fiber's GVD limits the bit rate to about 2 Gb/s for $L = 50$ km. This limitation can be overcome by employing the technique of dispersion management (see Chapter 8).

2.5 Fiber Losses

Power loss within a fiber link represents a major limiting factor because it reduces the signal's power reaching the receiver. As optical receivers need a certain amount of power for recovering the signal accurately, transmission distance is inherently limited by the fiber's losse. In fact, the use of silica fibers for optical communications became practical only when losses were reduced to an acceptable level during the 1970s. This section is devoted to a discussion of various loss mechanisms in optical fibers.